

## Supplementary information for:

### **Wulff in a cage gold nanoparticles as contrast agents for computed tomography and photoacoustic imaging**

Maryam Hajfathalian<sup>1</sup>, Ahmad Amirshaghghi<sup>2</sup>, Pratap C. Naha<sup>1</sup>, Peter Chhour<sup>2</sup>, Jessica C. Hsu<sup>2</sup>, Keely Douglas<sup>2</sup>, Yuxi Dong<sup>2</sup>, Chandra M. Sehgal<sup>1</sup>, Andrew Tsourkas<sup>2</sup>, Svetlana Neretina<sup>3</sup>, David P. Cormode<sup>1, 2\*</sup>

<sup>1</sup>Department of Radiology, <sup>2</sup>Department of Bioengineering, Perelman School of Medicine of the University of Pennsylvania, 3400 Spruce St, 1 Silverstein, Philadelphia, PA 19104, USA, Tel: 215-615-4656, Fax: 215-662-7868.

<sup>3</sup>College of Engineering, University of Notre Dame, Fitzpatrick Hall, Notre Dame, Indiana 46556, United States

[david.cormode@uphs.upenn.edu](mailto:david.cormode@uphs.upenn.edu)

\* Corresponding Author

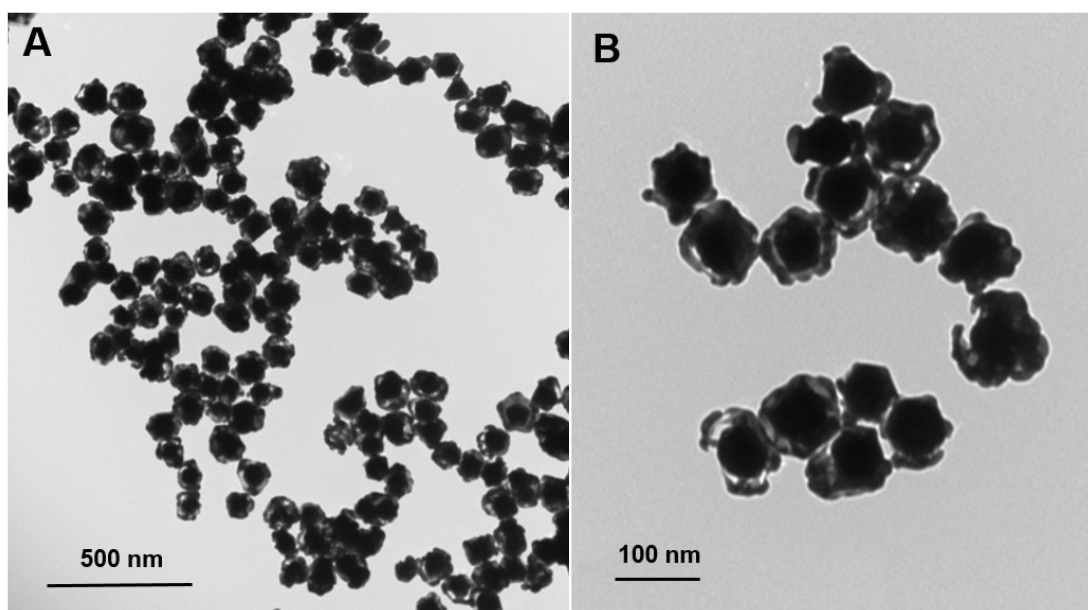


**Figure S1.** TEM of WICN that were formed using 12 ml of 300  $\mu\text{M}$  aqueous  $\text{HAuCl}_4$ , which resulted in fragmented shells (A and B are micrographs of the same sample presented at different magnifications).

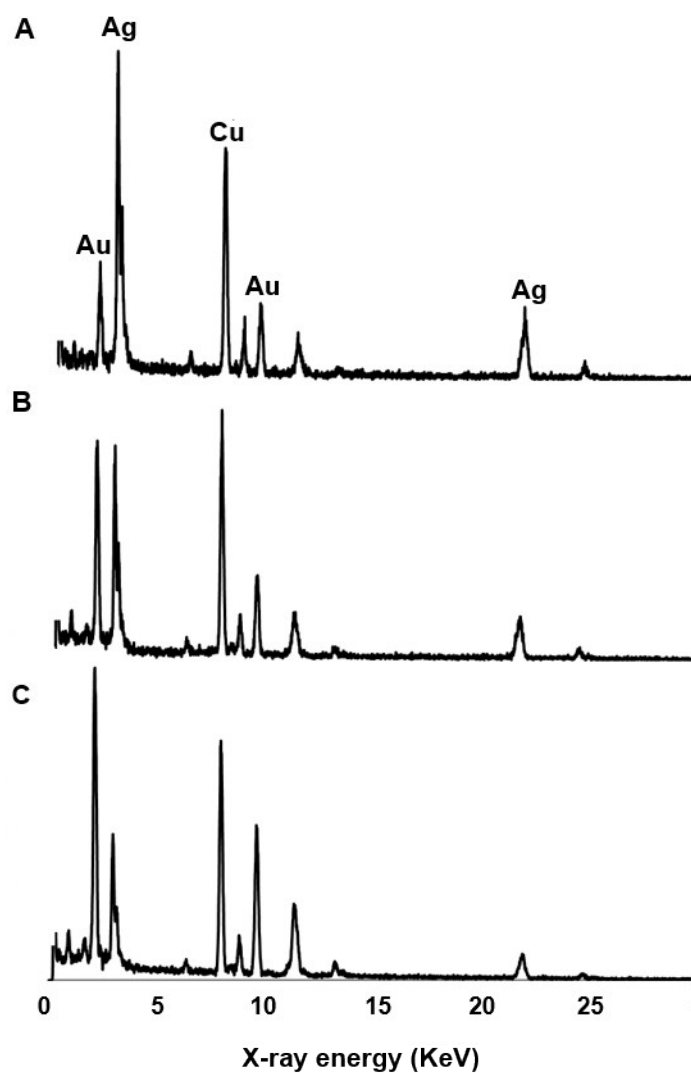


**Figure S2.** EDS spectra of Au-Ag nanoparticles at different stages of synthesis. A) Au@Ag core-shell structures. B) GRR of Ag with Au to form an AuAg nanoshell after adding 4 ml of 300  $\mu$ M HAuCl<sub>4</sub> C) WICN after adding 8 ml of 300  $\mu$ M HAuCl<sub>4</sub>. Note the increase in the height of the Au peaks relative to the Ag peaks as the GRR proceeds.

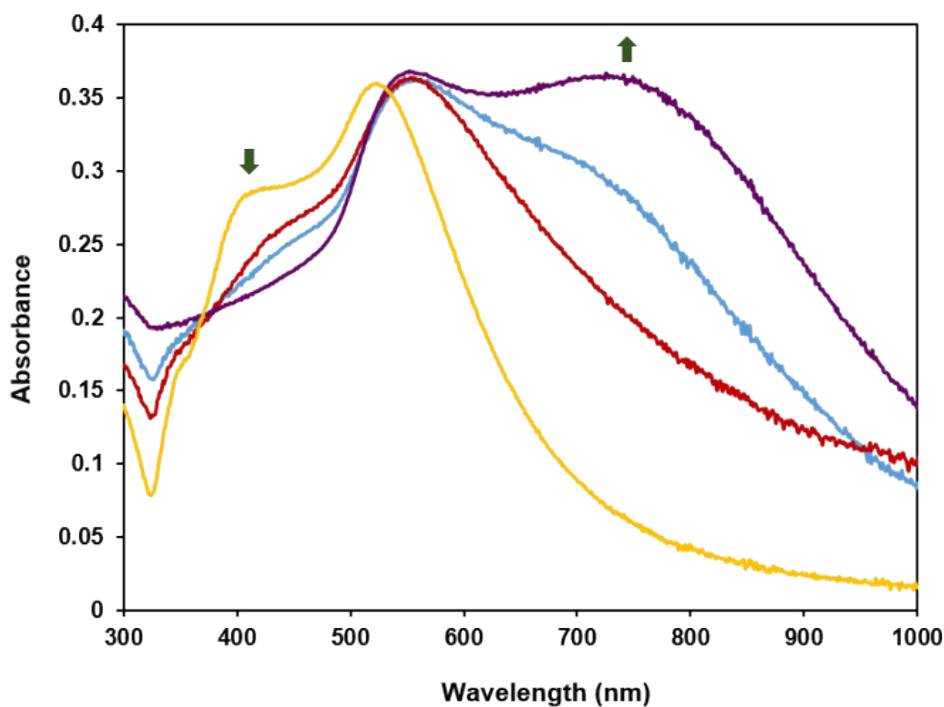


**Figure S3.** UV-vis absorption spectra of various nanoparticle formulations. The silver peak in Au@Ag core-shell structures (yellow line) decreased with the introduction of 4 ml of 300 uM HAuCl<sub>4</sub> into the solution (red line), Continuing the GRR with 6 ml of 300 uM HAuCl<sub>4</sub> results in the emergence of a second peak around 750 nm while the 400 nm peak further diminished (blue line). A strong peak in the NIR is distinguishable with the extent of GRR using 8 ml of 300 uM HAuCl<sub>4</sub> (purple line) utilized to form WICN (The green arrows show the decrease and increase in plasmon peak around 400 nm and 750 nm, respectively). The more gold chloride added (and hence more galvanic replacement occurring), the more the 400 nm peak of the silver shell declines, and the more prominent the peak at 750 nm that arises from the gold cage.

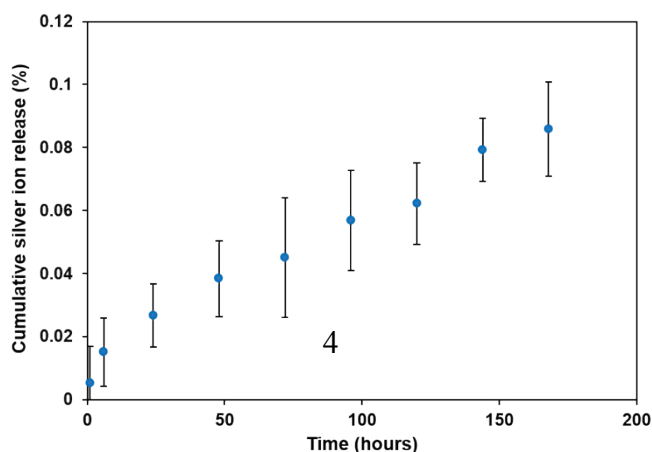


**Figure S4.** Silver ion release from WICN when incubated in DI water at 37 °C over a period of 7 days.

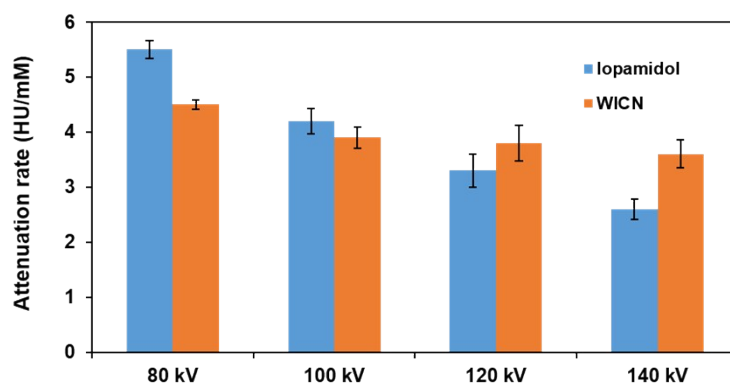


**Figure S5.** CT attenuation rates of Iopamidol and WICN at different X-ray energies.

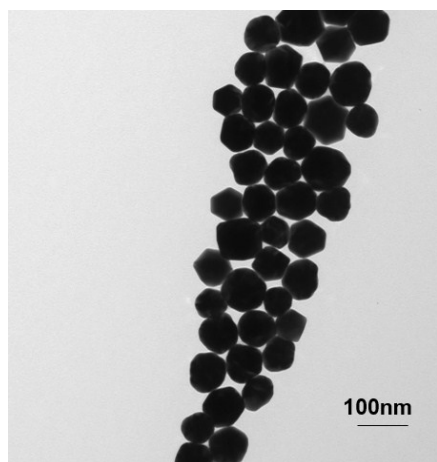


**Figure S6.** TEM of solid spherical AuNP with size similar to WICN.

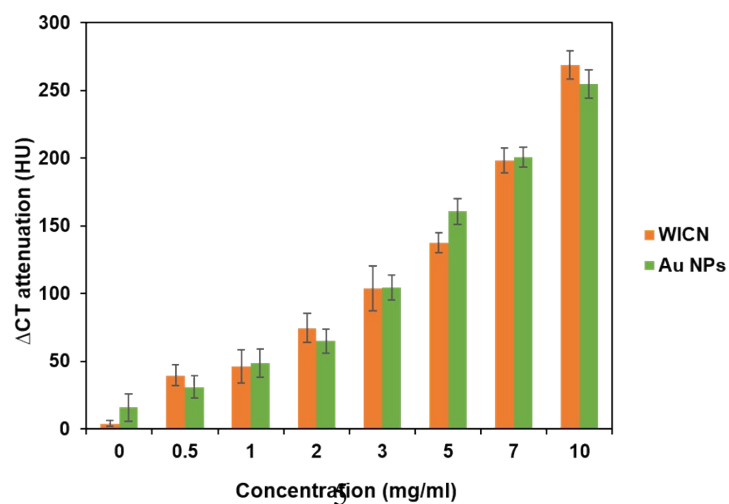


**Figure S7.** CT attenuation of WICN and solid spherical AuNP of a similar size at 80 kV.

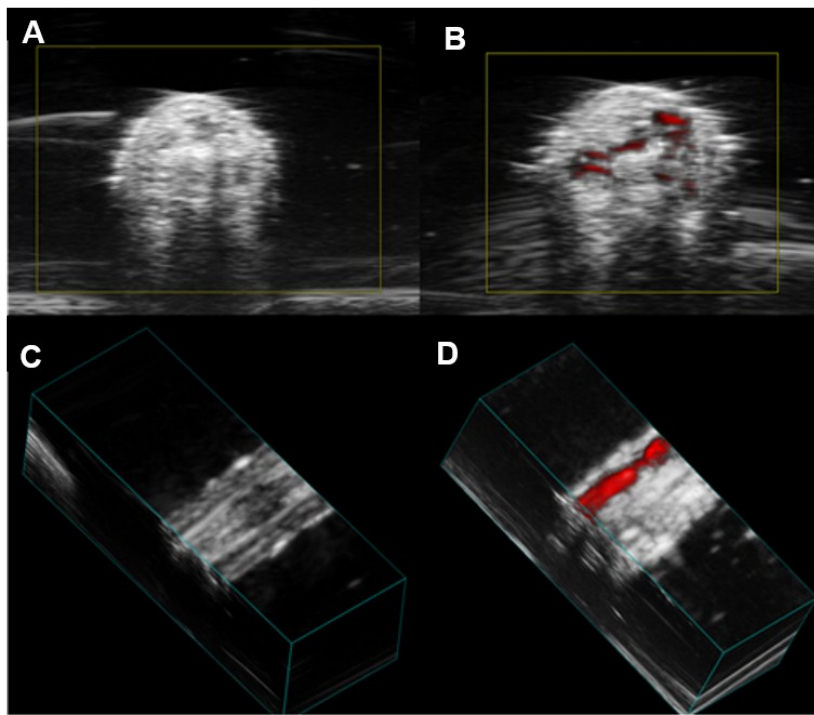


**Figure S8.** Cross-sectional PA images of a mouse tail A) before injection and B) immediately after injection of WICN. 3D images of the tail C) prior to and D) after injection of WICN.

**S9. link to Real-time movie of WICN injection**

<https://app.box.com/file/283680701038>

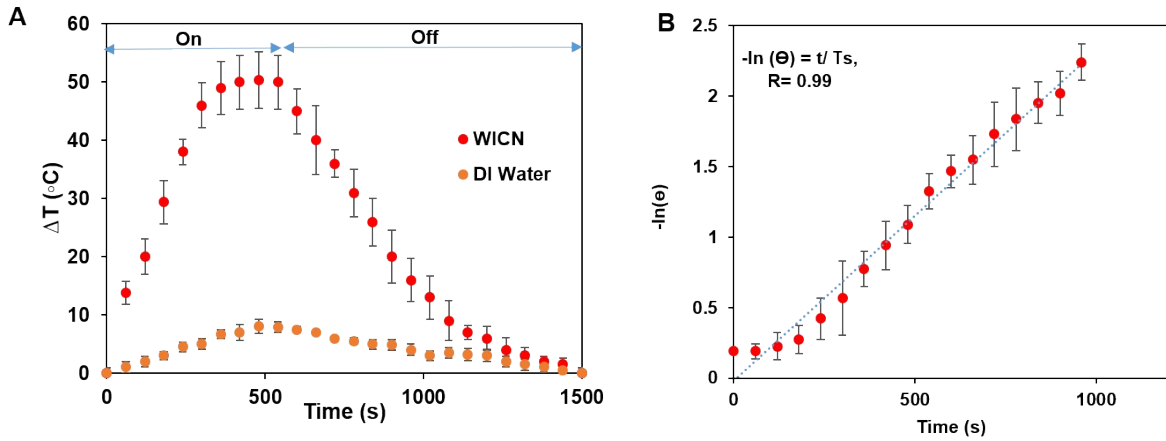


**Figure S10.** In vitro photothermal experiments using WICN. A) Heating and cooling curves of WICN (10 ug/ml) and DI water (at laser irradiation of 808 nm). The maximum temperature observed for the WICN solution was much higher than that for DI water. B) The linear regression between cooling period and  $-\ln(\theta)$  of driving force temperature from Figure S9A (Error bars are standard deviation of three WICN samples).

### Calculation of the photothermal conversion efficiency

The photothermal conversion efficacy of WICN was calculated using the following equation:

$$\eta = (hS\Delta T_{\max} - Q_s) / I(1 - 10^{-A_{808}}) \quad (1)$$

$$T_s = m_D C_D / hS \quad (2)$$

Where  $h$  is the heat transfer coefficient,  $S$  is the surface area of the container,  $T_{\max}$  is the maximum steady temperature of the solution of the WICN (i.e. 74.4 °C), and environmental temperature ( $T_{\text{Surr}}$ ) was 18 °C.  $I$  is the laser power (2 W),  $A_{808}$  is the absorbance of the WICN at 808 nm ( $A = 0.3$ ), and  $Q_0$  express heat absorbed by the quartz cell. The variable  $T_s$  is the sample-system time constant (Figure S 7B), and  $m_D$  and  $C_D$  are the mass (1 g) and heat capacity ( $4.2 \text{ J} \cdot \text{g}^{-1} \cdot \text{°C}^{-1}$ ) of the deionized water used as the solvent. From equations (1) and (2), the  $\eta$

value of the WICN was calculated to be 56%, which is higher than gold nanorings (42%)<sup>1</sup>, gold nanorod (21.3%)<sup>2</sup>, gold nanoshells (13%)<sup>3</sup>, graphene oxide (25%)<sup>4</sup>, Cys-CuS NPs (38%)<sup>2</sup> Au@Cu<sub>2-x</sub>S Core@Shell (52%)<sup>5</sup>.

### Calculation of the number of WICN in comparison with empty shell in same concentration

The metal volumes of empty cages, cores and WICN were calculated using the following equation:

$$V_{\text{Shell}} = 4/3\pi (R^3 - r^3) \quad (1)$$

$$V_{\text{Core}} = 4/3\pi Q^3 \quad (2)$$

$$V_{\text{WICN}} = V_{\text{Shell}} + V_{\text{Core}} \quad (3)$$

Where R is the outer radius (42 nm), r is the inner radius of cage (40 nm). The radius of the core (Q) was 34 nm. These values are obtained from TEM of the WICN. These calculations show we need to inject 4.9 times more empty cages rather than WICN to the mice to get the same signal. (To simplify the calculations, we assumed that the gold cage was spherical and we do not take into account the porosities of the cages).

### References

- 1 Y. Liu, Z. Wang, Y. Liu, G. Zhu, O. Jacobson, X. Fu, W. Fan, *ACS nano*, 2017, **11**, 10539.
  - 2 X. Liu, B. Li, F. Fu, K. Xu, R. Zou, Q. Wang, J. Hu, *Dalton transactions*, 2014, **43**, 11709.
  - 3 C. M. Hessel, V. P. Pattani, M. Rasch, M. G. Panthani, B. Koo, J. W. Tunnell, B. A. Korgel, *Nano letters*, 2011, **11**, 2560.
  - 4 D. Meng, S. Yang, L. Guo, G. Li, J. Ge, Y. Huang, J. Geng, *Chemical Communications*, 2014, **50**, 14345.
  - 5 H. Zhu, Y. Wang, C. Chen, M. Ma, J. Zeng, S. Li, M. Gao, *ACS nano*, 2017, **11**, 8273.
-